GEO Optical Data Association with Concurrent Metric and Photometric Information

Phan Dao[1] and Dave Monet[2]

[1] Air Force Research Laboratory, Kirtland AFB

[2] US Naval Observatory, Flagstaff Station

Abstract

Data association in a congested area of the GEO belt with occasional visits by non-resident objects can be treated as a Multi-Target-Tracking (MTT) problem. For a stationary sensor surveilling the GEO belt, geosynchronous and near GEO objects are not completely motionless in the earth-fixed frame and can be observed as moving targets. In some clusters, metric or positional information is insufficiently accurate or up-to-date to associate the measurements. In the presence of measurements with uncertain origin, star tracks (residuals) and other sensor artifacts, heuristic techniques based on *hard decision* assignment do not perform adequately. In the MMT community, Bar-Shalom [2009 Bar-Shalom] was first in introducing the use of measurements to update the state of the target of interest in the tracking filter, e.g. Kalman filter. Following Bar-Shalom's idea, we use the Probabilistic Data Association Filter (PDAF) but to make use of all information obtainable in the measurement of three-axis-stabilized GEO satellites, we combine photometric with metric measurements to update the filter. Therefore, our technique Concurrent Spatio-Temporal and Brightness (COSTB) has the stand-alone ability of associating a track with its identity –for resident objects. That is possible because the light curve of a stabilized GEO satellite changes minimally from night to night. We exercised COSTB on camera cadence data to associate measurements, correct mistags and detect non-residents in a simulated near real time cadence. Data on GEO clusters were used.

1. Introduction

For optical sensors, the first step in correlating space objects with a central catalog is to associate the detected signature with the corresponding orbital information. This task is trivial when there is only one unresolved blob in the field of view when the telescope is pointed to where an object is supposed to be according to its orbit. When more than one object exist in the field of view the common practice is to associate them according to their estimated positions. These non-probabilistic algorithms which rely on fixed positional boundaries for associating objects, work well in uncongested space. However, the population of objects has grown in size and it's common to find objects which are not anticipated by current orbital information. The GEO belt has the additional complication of localized congestion. That's particularly common for satellites in a GEO cluster because they occupy a narrow range of longitudes and they are actively kept in the slot by frequent station-keeping. As a result, orbital information often becomes obsolete as soon as or soon after an ephemeris is generated, which may result in cross-tagging in the catalog and corrupt metric and photometric data. The problem is also exacerbated when the signal from the object is weak and comparable to spurious noise. We use this particular system to demonstrate a new probabilistic technique to associate data. Our technique uses both positional and photometric information to associate data and label each detection with its most probable object's identity.

The problem of associating measurement data whose origin is uncertainty has been addressed abundantly in the research field of Multiple Target Tracking, mainly for radar. In particular, the review paper by Bar-Shalom [2009 Bar-Shalom] described in details the implementation of the Joint Probabilistic Data Association Filter (JPDAF) to track multiple radar targets in clutter. We applied a variant of the JPDAF to the electro-optical data for GEO space objects. For three-axis stabilized satellites, the light curve changes minimally from night to night. Therefore optical brightness can provide an additional verification of the satellite's identity. Our Concurrent Spatio-Temporal and Brightness (COSTB) technique is now implemented with JPDAF. The objectives is (a) associating and identifying resident objects and (b) detecting and tracking of non-resident objects. While COSTB is used to avoid cross-tags in GEO clusters, where multiple objects are always present in the field of view, it's also useful for detecting and tracking non-resident objects that momentarily drift in the field of a resident satellite.

2. Test data

To test and evaluate COSTB we use data collected on the Anik cluster at the longitude of 107º West. In September of 2014, the cluster consists of Anik F1 (NORAD #26624), Anik F1R (NORAD #28868), Anik G1 (NORAD #39127) and Echostar 17 (NORAD # 38551). Echostar 17 is nominally 0.2 deg from the other three satellites. In the collect, as seen in Fig. 1, the separation in apparent longitude between the Anik satellites are ~0.03 deg on average. This small angular separation represents a challenge, particularly for a wide field of view of a commercial lens. Knowing that there are 4 resident satellites in the field of view and additional objects may drift into the field, the six brightest blobs are recorded for each frame. For the purpose of this demonstration, the recorded blobs are unlabeled prior to the application of COSTB. The filter is operated with a maximum of 16 tracks. Each valid track is a hypothesis of a tracked object so there could be more tracks than observed blobs. Tracks can be joined, based on a user-defined threshold, if they are probabilistically indistinguishable. In other words, when it's determined that two equally probable tracks share the same data points, the one with a shorter history will be discarded. The threshold for discarding tracks is set low because in our application, clutter is not spatially correlated and cannot easily induce artificial tracks.

To test the filter with a stressing case, we choose the collects (nights) in the eclipse season, between September 22 and 26, for the test. Because data is missing when the satellites enter the shadow of the Earth and the filter will be required to associate the reappearing tracks using photometry. As seen in Fig. 1, the satellites' inclination (latitude) also reaches its highest point near eclipse. The turn-around trajectory corresponds to a deceleration and change of direction of the blob during the time when positional updates are unavailable, compounding the difficulty of the challenge.

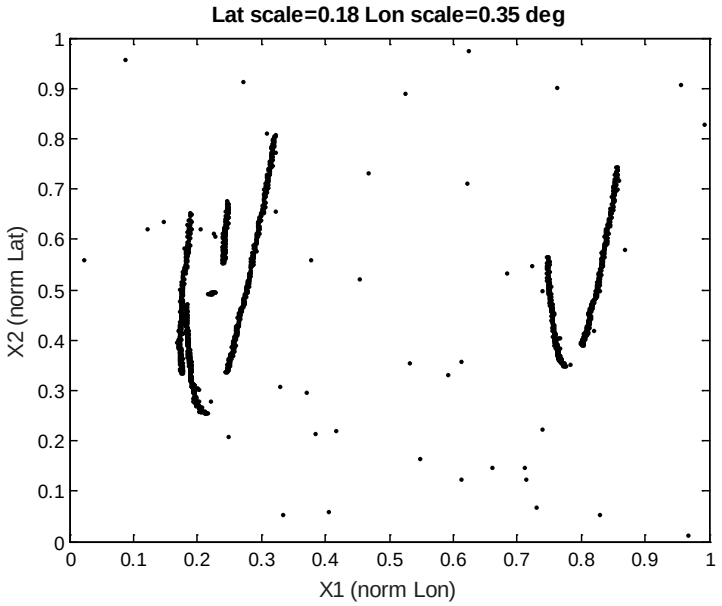

Figure 1. A zoomed-in field of detected signatures for the night of Sept-24-2014. The signature blobs are shown in normalized latitudes and longitudes. The full height and width and the shown sub-field are 0.18 and 0.35 degrees.

3. COSTB Technique

3.1 JPDAF

A description of the JPDAF filter is beyond the scope of this report. For details, refer to the review paper by Bar-Shalom [2009 Bar-Shalom]. It suffices to note that the association probabilities of the tracked object for each validated measurement are calculated each time and therefore the association is made "on-line" and COSTB can operate as a filter. Because computation time is small with respect to the time between consecutive measurements, the result is delivered in near real time. Probabilistic information is used by the algorithm to account for the measurement origin uncertainty. As shown next, a Kalman Filter can be used because the state and the measurement equations are almost linear. For the typical camera cadence, non-linear equations are not needed. However for systems with sparser cadence, Extended Kalman Filter could be used instead to account for non-linearity. We treat the problem as tracking multiple objects in a two dimensional space. The object's right ascension and declination are reduced to its apparent longitude and latitude. The following description provides some details on how to set up the KF. Typical KF notation is of course used. For the USNO camera frame interval, objects can be assumed to have a nearly constant velocity with state

$$x = [\lambda \ \phi \ \lambda \ \phi] \tag{1}$$

Velocity and acceleration changes are of course accounted for between time steps. If the current step is k, the state vector is predicted from step k-1

$$\hat{x}(k \mid k+1) = F(k-1)x(k-1 \mid k-1) \tag{2}$$

where the transition matrix $F = \begin{bmatrix} F_\lambda & 0 \\ 0 & F_\phi \end{bmatrix}$ is defined with $F_\lambda = F_\phi = \begin{bmatrix} 1 & T \\ 0 & 1 \end{bmatrix}$. The measurement is predicted ahead in time as

$$\hat{y}(k \mid k-1) = H(k)x(k \mid k-1) \tag{3}$$

with the observation matrix defined as $H = \begin{bmatrix} 1 & 0 & 0 & 0 \\ 0 & 0 & 1 & 0 \end{bmatrix}$.

the state covariance matrix *P* as

$$P(k \mid k-1) = F(k-1)P(k-1 \mid k-1)F(k-1)' + Q(k-1) \tag{4}$$

where $P(k-1 \mid k-1)$ is calculated according to the basic assumption of PDAF (Eq. 29 of Shalom [2009 Bar-Shalom]. *F* and *Q* are as follows for the case of maneuvering objects in clutter.

$$Q_\lambda(k) = \begin{bmatrix} T^4/4 & T^3/2 \\ T^3/2 & T^2 \end{bmatrix} \sigma_\lambda^2 \; or \; \begin{bmatrix} T^2/3 & T/2 \\ T/2 & 1 \end{bmatrix} T\,\sigma_\lambda^2$$

(5)

A similar expression for $Q_\phi(k)$ is also used to complete the definition of the overall Q:

$$Q(k) = \begin{bmatrix} Q_\lambda & \begin{matrix} 0 & 0 \\ 0 & 0 \end{matrix} \\ \begin{matrix} 0 & 0 \\ 0 & 0 \end{matrix} & Q_\phi \end{bmatrix}$$

(6)

The association compares the multi-variate Gaussian probability distance of measurement *x* to a user-selected gate level. The covariance matrix of the Gaussian density is the innovation covariance matrix of the correct measurements.

$$S(k) = H(k)P(k \mid k-1)H(k)' + R(k)$$

(7)

The state update equation of PDAF is

$$x(k \mid k) = \hat{x}(k \mid k-1) + W(k)\,\nu(k)$$

where the gain is the same as in standard KF $W(k) = P(k \mid k-1)H(k)'S(k)^{-1}$ and the PDAF combined innovation (or error) $\nu(k)$ is defined as in Eq. 40 of [2009 Bar-Shalom].

Fig. 2 describes a notional cycle of the association filter. In Fig. 2 $\tilde{P}(k)$ the spread of the innovations term as defined in Eq. 44 of [2009 Bar-Shalom].

We did not treat the position of the object as a three dimensional variable. That would allow us to relate its state to the ephemeris. We do not believe that an element set can be efficiently maintained in the presence of maneuvers and the benefit of 3D tracking is minimal and decide to use a 2D filter to reduce the dimensionality of the problem. A 3D JPDAF filter was reported by [2014 Stauch].

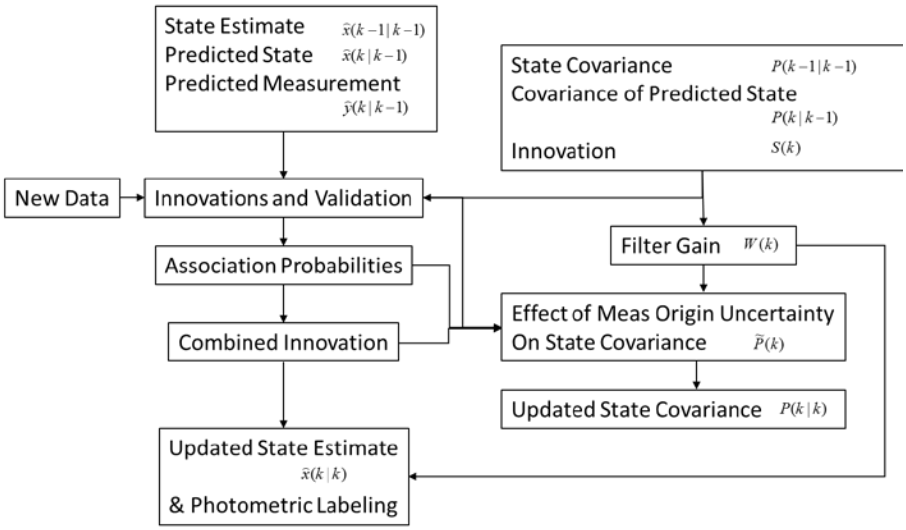

Figure 2. Diagram of data flow

3.2 Photometric association

To use photometric information for associating new measurements with satellite's identity, e.g. NORAD number, light curves are required. For each satellite, one expects that the brightness measured at a given time (or solar phase angle) can be approximated by recently recorded light curves. Previously recorded photometry is the baseline to which current brightness is compared. The brightness at a given time is estimated by past brightness measured at the same time. To prepare for the association, baseline photometry recorded on 22-Sep-2014 is used. This step is only required one time to kick off the test. In subsequent days, new photometry which will be associated by COSTB will serve as the new baseline. The technique to label photometry (to form initial baseline) without previous baseline was shown in [2016 Dao]. Baseline photometry for ANIK F1, ANIK F1R, ANIK G1 and ECHOSTAR 17 for 22-Sep-2014 is shown in Fig. 3. Note that photometric association is only effective when the magnitudes of the satellites are distinguishable. When the light curves overlap in magnitude, satellites' brightness are essential the same and cannot be used to distinguish one from another.

Photometric association is applied only on valid tracks maintained by the JPDAF filter. For each measurement an overall score is calculated for the purpose photometric association. For an ordered list of observed magnitudes, all permutations of baseline magnitudes (satellite's identity) are considered. For each permutation, the sum of the absolute magnitudes of the differences between measurement and baseline is calculated. The permutation with the smallest sum is selected as the most likely association and a score is calculated.

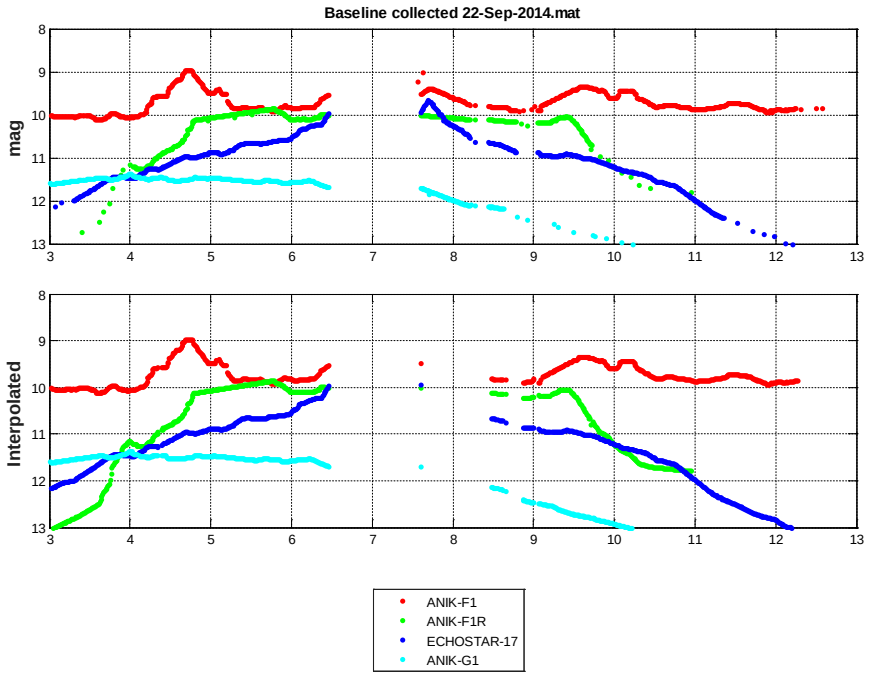

Figure 3. Baseline photometry collected 22-Sep-2014 are shown in the upper plot. Expected magnitudes for the four listed satellites are shown in the lower plot for the observation times on 24-Sep-2014.

While real time association may not be possible when the brightness values of different satellites are indistinguishable, satellite identity can still be assigned based on track/positional information. We make use of the fact that blobs belonging to the same well-established track should be associated to the same satellite and therefore be given the same identity. There are of course exceptions to that rule. When there is a substantial measurement lapse, for example due to the eclipse of the satellites, old tracks are terminated and new tracks generated. In our algorithm, the new tracks are not related to the old tracks. One cannot extend photometric association across the gap of data and the first few measurements after the eclipse cannot be associated right away.

4. Results and discussions

The results of running COSTB on 24-Sep-2014 data for real time association is shown in Fig 4. We will compare Fig 4 and the plot of unassociated data in Fig 5. The large gap of associations between 6:25 and 8:45 UTC is comparable but slightly wider than the gap in the unassociated data shown in Fig 5. Because of the absence of measurement during eclipse, the tracks are terminated and when observation resumes at approximately 8:25 new tracks are generated. The magnitudes of Anik-F1 (red in Fig 4) and Echostar-17 (blue in Fig 4) are well separated at that time so we anticipate the association to start working right away. However, the association doesn't resume until 8:45 because the tracks are interrupted by a second gap of data between 8:34 and 8:45, evident in Fig. 5.

Between 3:15 to 4:15 UTC, there are small gaps of association. These gaps are attributed to the overlap between the expected values of magnitude, seen in Fig 3 as "crossing" of the three impacted satellites around 4 UTC. The gaps in association are commonly due to the lack of separation in magnitudes at the time when the track history is not long enough. The required history's length is selected by the user as a minimum number of validated track points.

The obvious mis-association of Echostar-17 near 10:40 UTC, when some of the Echostar-17 signatures are erroneously attributed to Anik-F1R, can be due to the crossings of magnitude seen in the observed light curves (Fig.

5) as well as in the expected light curves (Fig. 3). In future implementation, once photometric identity is established, the previous points in an established track will be relabeled with the new identity if they have not been already labeled. That would improve the accuracy of time-delayed association but not the on-line near real time association shown in Fig. 4.

While we only present results of associating measured signatures with baseline photometry, COSTB also generates tracks and photometry of non-resident objects that cross the field of view. To be able to identify the resident signatures also allows us to recognize the signatures of the non-residents.

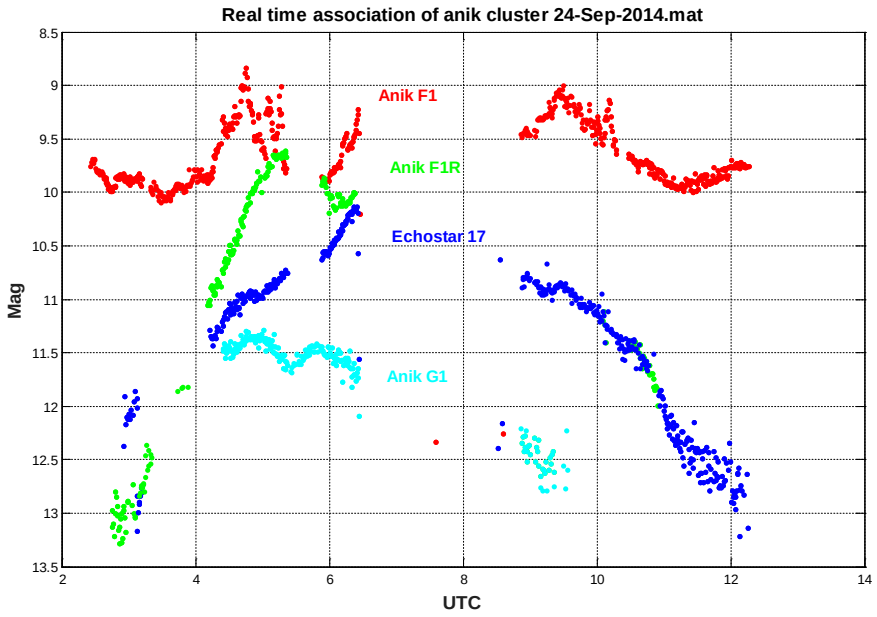

Figure 4. The visual magnitudes of detected and on-line associated signatures are shown as color-coded dots.

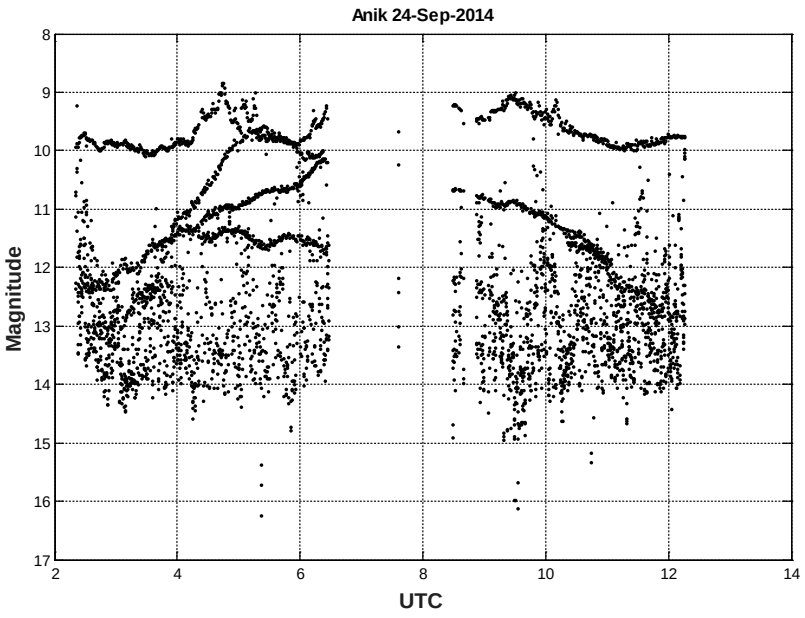

Figure 5. Unassociated photometry of multiple objects in the Anik cluster.

5. Conclusion

We demonstrated that on-line near real-time association of optical signatures collected by a high cadence and wide field of view camera system can be accomplished by the JPDAF filter with photometric data augmentation. The filter is set up on top of a Kalman filter that treats the satellite's signatures as targets moving in a two dimensional space with possible maneuvers. The filter codes are implemented in COSTB and tested against the challenging Anik cluster data set. We also tested the operation of COSTB across the eclipse gap of measurements and studied the recovery of the filter. We are encouraged by the qualitative evaluation of the results. We recommend the implementation of COSTB for tracking satellites in congested areas of the GEO belt.

Acknowledgements

We acknowledged the support of the SpaceCraft Object Tracking and Characterization program and its program manager Virginia Wright. Jason Baldwin and Tom Kelecy have inspired this work and helped us understand the use of JPDAF in their Constrained Admissible Region-Multiple Hypothesis Filter (CAR-MHF) codes.

References

[2009 Bar-Shalom] Yaakov Bar-Shalom, Fred Daum and Jim Huang, The probabilistic data association filter, IEEE Control Systems, Volume: 29 Issue: 6, 2009.

[2014 Stauch] J. Stauch, M. Jah, J. Baldwin, T. Kelecy, and K. Hill, *Mutual application of joint probabilistic data association, filtering, and smoothing techniques for robust multiple space object tracking*, in Proceedings of the AIAA/AAS Astrodynamics Specialist Conference, no. AIAA-2014-4365, Aug. 2014.

[2016 Dao] Phan Dao, Elisabeth Heinrich-Josties and Todd Boroson, *Automated Algorithms to Identify Geostationary Satellites and Detect Mistagging using Concurrent Spatio-Temporal and Brightness Information*, 2016 AMOS.